Original Research Paper

Ultrasound-Assisted Enzymatic Extraction of Polysaccharides from Waste Corn Bract: Process Optimization, Characterization, Antioxidant and Anti-Diabetic Potentials

[1]Yihui Liu, [1]Yayi Li, [2]Na Niu, [1]Yuxing Xie, [1]Wangyou Zhang, [1]Shuaiyi Dong, [1]Gulei Pu, [1]Chenqi Liu, [1]Caibo Jiang, [1]Mingjin Cai, [1]Yang Liu and [1]Yang Zhang

[1]*Department of Biology and Food Engineering, Changshu Institute of Technology, China*
[2]*Department of Microbiology Laboratory, Food Inspection and Quarantine Technology Center of Shenzhen Customs District, China*

Abstract: Corn bract is the main agricultural waste of corn production and processing. Little information is focused on its value-added utilization. In the present study, the Ultrasound-Assisted Enzymatic Extraction (UAEE) was used for the first time to extract Corn Bract Polysaccharides (CBPs). The optimum conditions of UAEE for CBPs extraction were: Cellulase amount of 0.7%, enzymolysis for 58 min, and ultrasound treatment for 30 min at 729 W, under which the CBPs yield reached $1.17\pm0.06\%$, significantly higher than other methods. CBPs are composed of ribose, rhamnose, glucuronic acid, galacturonic acid, glucose, galactose, xylose, arabinose, and fructose at molar ratios of 3.82: 4.25: 3.54: 8.11: 32.89: 1.00: 27.96: 12.57: 13.25 and have a molecular weight of 215.7 kDa and a particle size of 255 nm. The surface of CBPs appears to be full of holes and bumps and the infrared spectroscopic analysis confirmed that CBPs possess the typical characteristics of polysaccharides and could be a kind of naturally occurring sulfated polysaccharides. CBPs extracted with the optimized UAEE preferentially scavenge reactive nitrogen species with IC_{50} of 1.76 ± 0.14 mg.mL^{-1} for scavenging hydroxyl radical and have medium inhibitory effects on α-glucosidase with IC_{50} of $20.66\pm0.98\%$ mg.mL^{-1}. The present contribution provides an efficient UAEE method to obtain the CBPs with antioxidant and anti-diabetic potentials. It will give a useful clue for the comprehensive and value-added exploitation of waste corn bract.

Keywords: Corn Bract, Polysaccharides, Ultrasound-Assisted Enzymatic Extraction, Antioxidant Capacity, Anti-Diabetic Potential

Introduction

Corn, also known as *Zea mays* L. belonging to the Poaceae family, is a common grain crop distributed all over the world (Gesteiro *et al.*, 2021). Except for edible use, some corn-based wastes have been fully utilized. For example, the corn stigma and style (corn silk) are rich in vitamins, polysaccharides, flavonoids, alkaloids, steroids, and tannins (Peng *et al.*, 2016) and exert diverse health benefits, including antioxidant, anticoagulant, anti-cancer, diuretic and hypoglycemic properties (Zhao *et al.*, 2017). Thus, corn silk is commonly consumed in various nutraceuticals and functional foods (Hasanudin *et al.*, 2012). However, corn bract, the subtending leaf surrounding corn kernel that accounts for 40% per unit area of corn has received little attention and open burning is usually performed to dispose of the waste corn bract

(Luo *et al.*, 2017). In previous research, we found that total flavonoids from corn bract possess promising antioxidant and antibacterial capacities (Zhang *et al.*, 2019). It is suggested that corn bract would be a new natural source to discover nutraceuticals and pharmaceuticals. Thus, waste corn bract deserves in-depth study to promote its value-added utilization.

Polysaccharides also called glycans (Yang *et al.*, 2019), are a kind of macromolecules consisting of various monosaccharides connected by glycosidic bonds (Vo and Kim, 2014). Recently, natural polysaccharides have attracted great interest owing to health-promoting functions, particularly for immuno-enhancement, antioxidant and hypoglycemic properties (Ji *et al.*, 2017). Traditionally, polysaccharides are usually extracted with hot water, alkaline, and acidic extractions, but these extraction methods suffer from the disadvantages of high

temperature, long time, high extraction temperature, and low yield. Currently, some emerging techniques, including enzyme-assisted extraction, ultrasound-assisted extraction, microwave-assisted extraction, and combined technologies have been successfully used to extract polysaccharides from natural materials efficiently (Zhang *et al*., 2021). The Enzyme-Assisted Extraction (EAE) is focused on accelerating the release of bio components via degrading plant materials (Chen *et al*., 2011), of which the cellulase is most frequently applied to targeted decompose the celluloses that are composed of the cell walls, thereby enhancing the release of ingredients from the inside of cells (Fu *et al*., 2008). Moreover, the Ultrasound-Assisted Extraction (UAE) is another green extraction technique and its cavitation effects can produce high shear forces in the media, thus facilitating the delivery of energy (Chemat *et al*., 2017). The Ultrasound-Assisted Enzymatic Extraction (UAEE) combines the advantages of UAE and EAE and has been applied to extract high-yield polysaccharides from pumpkin (Wu *et al*., 2014), *Eleocharis dulcis* (Zhang *et al*., 2022) and *Setaria viridis* (Li *et al*., 2016). However, as far as we know, no research publications are available on the UAEE of Corn Bract Polysaccharides (CBPs).

Oxidative stress is mainly induced by the excessive generation of Reactive Oxygen Species (ROS), which can automatically oxidize proteins, lipids, and DNA to cause a series of chronic diseases (Ni *et al*., 2022; Zhang *et al*., 2021). Increasing evidence has highlighted the role of oxidative stress in deteriorating diabetes. The overproduced ROS can cause insulin resistance and β-cell dysfunction (Andreadi *et al*., 2022). Thus, it is essential to regularly replenish antioxidants for the prevention and adjuvant therapy of diabetes. Previous findings demonstrated that the antioxidant polysaccharides have great potential for the treatment of diabetes (Jiang *et al*., 2022; Wang *et al*., 2020), indicating that it is reasonable and feasible to explore the antioxidant and anti-diabetic properties of natural polysaccharides.

In the present investigation, the UAEE was conducted to extract CBPs for the first time. The extraction process was optimized by Response Surface Methodology (RSM)-Box-Behnken Design (BBD). Then, the CBPs extracted under the optimal conditions of UAEE were purified and characterized. Finally, the antioxidant and anti-diabetic potentials of purified CBPs were assessed. Herein, this study would provide evidence for the functional and medicinal utilization of waste corn bract.

Materials and Methods

Materials and Reagents

Corn bract was collected at a local market of agricultural products on 8 July 2021, Changshu, Jiangsu, China, and identified by Dr. Yang Liu, School of Biology and Food Engineering, Changshu Institute of Technology,

Changshu, Jiangsu, China. Corn bract was dried at about 60°C and pulverized to 60 mesh.

The cellulase with an activity of 10000 U.g^{-1} was bought from Macklin Biochemical Co., Ltd. (Shanghai, China). The L-Ascorbic Acid (LAA), acarbose, α-glucosidase with an activity of 50 U.mL^{-1}, 4-Nitrophenyl-β-D-Galactopyranoside (PNPG) and 1, 1-Diphenyl-2-Picrylhydrazyl (DPPH) were from BioDuly Co., Ltd. (Nanjing, Jiangsu, China). The monosaccharide standards, T-series Dextrans, and Diethylaminoethyl (DEAE) cellulose were from Yuanye Bio-Technology Co., Ltd (Shanghai, China). Other reagents with an analytical grade were obtained from Sigma Chemical Co., Ltd (St. Louis, MO, USA).

Study Design

According to the principles and flowcharts of experimental design reported in previous works (Ismy *et al*., 2022; Chzhu *et al*., 2020; Umana *et al*., 2020), a schematic diagram of the present study was drawn and presented in Fig. 1. Dried corn bract was grinded into powders with 60 mesh, then subjected to a UAEE to obtain CBPs. Based on the results of single-factor experiments, a four-variable-three-level RSM-BBD was performed to optimize the UAEE of CBPs. Afterward, the crude CBPs extracted under the optimal conditions were purified by a series of procedures, including deproteinization, DEAE column chromatography, and dialysis. Then, the purified CBPs were characterized by various procedures, including the determination of monosaccharide and molecular weight, particle size measurement, FT-IR analysis, and SEM observation. Meanwhile, the antioxidant capacities of purified CBPs were evaluated using DPPH and hydroxyl radicals as the testing models, and the anti-diabetic activity was assessed using α-glucosidase as the biomarker. The data were represented as means ± SD (standard deviation) and statistical analysis was tested with SPSS19.0 software (SPSS Inc., Chicago, USA).

UAEE of CBPs

One gram of degreased corn bract powders was dispersed in distilled water at a liquid-to-solid ratio of 40: 1 mL.g-1 for 2 h, adjusted pH to around 5.0, added certain amounts of cellulase (0.3-0.8%, relative to the solid materials) and incubated at 50°C for 40-90 min. After inactivating cellulase, the mixture was neutralized and transferred into an XH-300 UL Microwave/ultrasound extraction apparatus (Xianghu Technology Development Co., Ltd, Beijing, China), then subjected to an ultrasound treatment at different powers (400-900 W) for different durations (10-60 min). The mixture was filtered, condensed to ¼-1/5 of the original volume, and subjected to ethanol precipitation at 4°C for 12 h, then the crude CBPs were obtained by centrifugation and lyophilization (Li *et al*., 2016; Wu *et al*., 2014).
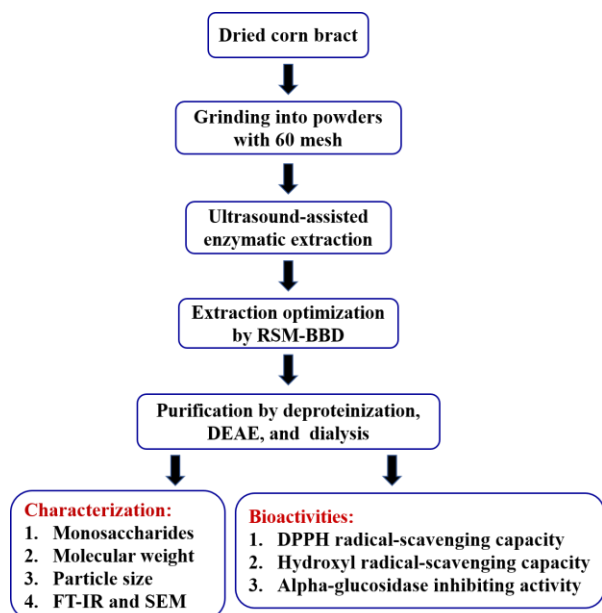
Fig. 1: Schematic diagram of the study. RSM-BBD: Response Surface Methodology-Box-Behnken Design; DEAE: Diethylaminoethyl; FT-IR: Fourier Transform-Infrared; SEM: Scanning Electron Microscopy; DPPH: 1, 1-Diphenyl-2-Picrylhydrazyl

The polysaccharides content in CBPs was quantified by the phenol-sulfuric acid method (glucose served as the standard) (Dubois *et al*., 1956). The standard curve was:

$$A = 7.3928C + 0.0085 \left(R^2 = 0.9998 \right) \tag{1}$$

where, A-absorbance and C-polysaccharides concentration (mg.mL^{-1}). The linear range was from 0.2 to 1.2 mg.mL^{-1}.

The CBPs yield was calculated according to the following formula:

$$Y(\%) = (C \times V \times D) / M \times 100 \tag{2}$$

where, Y-CBPs yield, C-polysaccharides concentration (mg.mL^{-1}), V-volume of the filtrate (mL), D-dilution factor, and M-weight of corn bract powders (mg).

Single-Factor Experiments

Four factors, including cellulase amount (0.3-0.8%), incubation time (5-10 min), ultrasound power (400-900 W), and ultrasound time (20-70 min) were elected to evaluate their effects on CBPs yield. For each experiment, when one factor varied, others were fixed.

Response Surface Methodology Optimization

Response Surface Methodology (RSM) (Azcarate *et al*., 2020) coupled with Box-Behnken Design (BBD) was used to achieve a four-variable-three-level project according to the results derived from the single-factor experiment (Table 1). The RSM analysis was performed with a Design Expert software version 8.0.6 (Stat-Ease, Inc., Minneapolis, USA). The validation was performed to testify to the accuracy of a model to predict the UAEE of CBPs and comparison experiments were implemented to explore the contributions of cellulase and ultrasound to the CBPs yield, respectively.

The regression analysis was fitted to the following second-order polynomial equation:

$$Y = \beta_O + \sum_{i=1}^{4} \beta_i X_i + \sum_{i=1}^{4} \beta_{ii} X_i^2 + \sum_{i=1}^{3} \sum_{j=i+1}^{4} \beta_{ij} X_i Y_j \tag{3}$$

where, The response; β_0-the intercept; β_i, β_{ii}, and β_{ij}- the coefficients of linear, quadratic, and interactive terms, respectively; X_i and X_j-independent variables.

Purification of Crude CBPs

The crude CBPs were deproteinized three times by the sevag reagent, then subjected to a DEAE column chromatographic purification using 0.5 m NaCl solution as eluent. Different fractions were gathered, condensed, and dialyzed to remove the ions and small-molecular-weight impurities. Finally, a freeze-drying process was performed to obtain the purified CBPs (Wei *et al*., 2019).

Characterization of Purified CBPs

Monosaccharide

The monosaccharides of CBPs were detected by High-Performance Liquid Chromatography (HPLC). In brief, 2 mg of purified CBPs were dissolved in 2 mL of 2 m Trifluoroacetic Acid (TFA) and heated at 110°C for 5 h. After removal of residual TFA, the mixture was dissolved in 200 μL of 0.3 m NaOH and mixed with 200 μL of methanol containing 0.5 mol.L^{-1} 1-Phenyl-3-Methyl-5-Pyrazolone (PMP), followed by reacting at 70°C for 1.5 h. After cooling, the reaction mixture was adjusted to pH 7.0 and extracted with chloroform. After the removal of chloroform, the PMP-labeled monosaccharides of CBPs were obtained.

Table 1: The variables and levels for RSM optimization.

Variables	Levels		
	-1.0	0.0	1.0
Cellulase amount (%, X$_1$)	0.6	0.7	0.8
Incubation time (min, X$_2$)	50.0	60.0	70.0
Ultrasound power (W, X$_3$)	600.0	700.0	800.0
Ultrasound time (min, X$_4$)	20.0	30.0	40.0

The analysis was conducted using an Ultimate 3000 High-performance liquid chromatograph (Thermo, Waltham, MA, USA) equipped with a Supersil ODS2 column (4.6 × 250 mm², 5 μm) and a diode array detector. The analytical conditions were: Column temperature-30°C, detection wavelength-245 nm, flow rate-0.8 mL.min-1, run rate-40 min and the mobile phase-0.05 m PBS (pH 6.8): Acetonitrile -82: 18 (*v/v*) (Hu *et al*., 2019).

Molecular Weight

The molecular weight was measured by High-Performance Size Exclusion Chromatography (HPSEC). Accordingly, the purified CBPs were dissolved in ultrapure water at a concentration of 1 mg.mL^{-1}, then filtered via a Millipore filter. A 1260 Infinity II High-performance liquid chromatograph (Agilent, Palo Alto, CA, USA) equipped with a TSK-gel G4000 PWXL column (7.8 mm × 300) was served as the analyzer. The analytical conditions were: Column temperature-50°C, column temperature-50°C, mobile phase-ultrapure water, detector temperature-30°C, flow rate-1.0 mL.min^{-1}, and run rate-30 min (Hu *et al*., 2019).

Particle Size

The particle size of purified CBPs was estimated by a Zetasizer Nano ZS900 Nanoparticle size analyzer (Malvern Instruments Co., Ltd., Malvern, United Kingdom) at a concentration of 1.0 mg.mL^{-1} (Krishnamoorthi *et al*., 2022).

Fourier Transform-Infrared (FT-IR) Spectroscopy

Two milligrams of dried powders of purified CBPs were ground with 200 mg of dried KBr and pressed into a pellet. A 650 FT-IR Spectrophotometer (Gangdong Sci. and Tech. Co., Ltd, Tianjin, China) was served to detect the absorption peaks ranging from 400 to 4000 cm^{-1} (Krishnamoorthi *et al*., 2021).

Scanning Electron Microscopy (SEM)

Approximately ten milligrams of dried powders of purified CBPs were loaded on a silicon pellet and carefully sputtered with thin layers of gold powders under reduced pressure. The SEM observation was conducted with a Regulus 8100 Scanning electron microscopy (Hitachi, Tokyo, Japan) with an accelerating voltage of 1.0 kV and the image magnification was fixed at 450 × (Krishnamoorthi *et al*., 2021).

The in Vitro Antioxidant Potentials of Purified CBPs

DPPH Radical-Scavenging Capacity

The purified CBPs were formulated into solutions at concentrations ranging from 0 to 5 mg.mL^{-1}. Then, 2 mL of CBPs solution were blended with 2 mL of ethanol containing 0.1 mm DPPH and reacted at 25° for 30 min and the absorbance at 517 nm (A_s) was recorded. The mixture lacking DPPH was employed as the normal control (A_c) and the mixture without CBPs served as the blank control (A_0). LAA was used as the positive control. The DPPH radical-scavenging rate was calculated according to the following equation (Zhang, *et al*, 2018):

$$DPPH\ radical-scavenging\ rate(\%)=(A_s-A_c)\times100/A_0 \quad (4)$$

Hydroxyl Radical-Scavenging Capacity

The purified CBPs were formulated into solutions at concentrations ranging from 0 to 5 mg.mL^{-1}. Then, 2 mL of CBPs solution were taken out and mixed with 1 mL of 0.75 mm 1, 10-phenanthroline PBS solution (pH 7.4), 1 mL of 0.75 mm FeSO$_4$ solution and 1 mL of 0.12% (*v/v*) H$_2$O$_2$ solution. After incubating at 37°C for 60 min, the absorbance at 536 nm (A_s) was measured. The mixture lacking H$_2$O$_2$ was served as the normal control (A_c) and the mixture lacking CBPs was used as the blank control (A_0). LAA was used as the positive control. The hydroxyl radical-scavenging rate was calculated according to the following formula (Zhang *et al.*, 2018):

$$Hydroxyl\ radical-scavenging\ rate(\%)$$
$$=(A_s-A_0)\times100/(A_c-A_0) \quad (5)$$

The Inhibitory Effects on α-Glucosidase Activity

The purified CBPs were formulated into different solutions ranging from 0 to 50 mg.mL^{-1}. Twenty microliters of CBPs solution were mixed with 40 μL of α-glucosidase solution and incubated at 37°C for 10 min. Then, 20 μL of 10 mm PNPG solution was added, followed by incubating at 37°C for 30 min. After that, 100 μL of 0.2 M Na$_2$CO$_3$ solution was added to cancel the reaction. The absorbance at 405 nm was determined and acarbose (0-5 mg.mL^{-1}) was served as the positive control. The inhibition rate of α-glucosidase was calculated as follows (Lv *et al.*, 2021):

$$Inhibition\ rate(\%)\ =\ \left[1-(A_1-A_2)/A_0\right]\times100\% \quad (6)$$

where, A_0 is the absorbance of PBS without CBPs; A_1-the absorbance of the mixture containing CBPs and PNPG; A_2-the absorbance of CBPs without PNPG.

Statistical Analysis

Statistical analysis was performed with the Statistical Product Service Solutions (SPSS) software (version 19.0) (SPSS Inc., Chicago, USA) and one-way analysis of variance (ANOVA) was applied to assess the significance. The $P<0.05$ was deemed as a significant difference.

Results and Discussion

Single-Factor Experiment

Before process optimization, four factors, including cellulase amount, incubation time, ultrasound power, and ultrasound time were selected to assess their effects on CBPs yield and to explore the proper variables and levels.

As shown in Fig. 2A, the yield of CBPs was elevated within the cellulase amount of 0.3-0.7%. After that, CBPs yield was decreased with the heightening of cellulase. The results suggested that cellulase potentiates the release of CBPs by degrading cell walls. However, excessive cellulase might make the medium more viscous, hindering the implementation of enzymolysis (Huang *et al*., 2016). Figure 2B exhibited the impacts of incubation time on CBPs yield. It can be noted that CBPs yield was increased with the prolongation of incubation time within the range of 40-60 min, when it exceeded 60 min, CBPs yield began to drop off. The results indicated that too long incubation time was not beneficial to increasing CBPs yield and the cellulase activity would decline, which was consistent with the phenomenon that had been found in our previous work (Zhang *et al*., 2019). Figure 2C described the effects of ultrasound power on CBPs yield. It can be observed that CBPs yield was improved with the increase of ultrasound power from 400 to 700 W, due to the increase in cavitation bubbles and mass transfer rates (Mason *et al*., 2011). When the power was further enhanced, CBPs yield was decreased, which may be related to the fact that high-powered ultrasound treatment can cause the depolymerization and/or aggregation of extractable polysaccharides, resulting in a decrease in CBPs yield (Chen *et al*., 2012). Similarly, with the continuous extension of ultrasound time after 30 min, CBPs yield began to fall (Fig. 2D).

To sum up, 0.7% cellulase, enzymolysis for 60 min, and ultrasound treatment at 700 W for 30 min were selected for the RSM-BBD design.

Model Fitting and Statistical Analysis

Based on the results of a single-factor experiment, four variables, including cellulase amount (X_1), incubation time (X_2), ultrasound power (X_3), and ultrasound time (X_4) were further optimized by RSM-BBD with CBPs yield as the response (Y). As shown in Table 2, 29 different schemes were obtained and the results were fitted with a second-order polynomial equation (Eq. 7). The CBPs yield varied from 0.48 to 1.15% and the maximum yield was achieved under the conditions of X_1 = 0.7%, X_2 = 60 min, X_3 = 700 W and X_4 = 30 min.

The second-order polynomial equation was:

$$\begin{aligned}
Y = {}& 1.1 + 0.0092\,X_1 - 0.037\,X_2 + 0.16\,X_3 + 0.0025\,X_4 \\
& + 0.015\,X_1X_2 + 0.035\,X_1X_3 - 0.11\,X_1X_4 + 0.08\,X_2X_3 \\
& - 0.013\,X_2X_4 - 0.047\,X_3X_4 - 0.18\,X_1^2 - 0.11\,X_2^2 \\
& - 0.27\,X_3^2 - 0.18\,X_4^2
\end{aligned} \tag{7}$$

where, Y-CBPs yield, X_1-cellulase amount (%), X_2-incubation time (min), X_3-ultrasound power (W), and X_4-ultrasound time (min).

The ANOVA results of the response surface quadratic model for CBPs extraction were presented in Table 3. It can be observed that a significant difference was found in the model ($P<0.01$) and no significant difference was noted in lack of fit ($P>0.05$), suggesting that this model is accurate for the prediction of CBPs extraction (Zhang *et al*., 2019). The Adj R^2 was 0.9432, indicating that 94.32% of the results can be covered and interpreted by the present model. The linear parameters X_2 and X_3 were significant ($P<0.05$ or $P<0.01$), but X_1 and X_4 were not significant ($P>0.05$). The interaction parameters X_1X_4 and X_2X_3 were highly significant ($P<0.01$), while X_1X_2, X_1X_3, X_2X_4, and X_3X_4 were not significant ($P>0.05$). The quadratic parameters X_1^2-X_4^2 were all notably significant ($P<0.01$).

The 2D contour and 3D response surface plots derived from Design Expert software can facilitate the visualization of interactions between different variables (Wei *et al*., 2019). As shown in Fig. 3A-3F, the interaction terms X_1X_4 and X_2X_3 exhibited more prominent influences on CBPs yield than those of the other interaction terms, which was in line with the results of the ANOVA analysis (Table 3). In addition, from Fig. 3G-3L, it can be noted that the CBPs yields were first raised and then reduced with the elevation of cellulase amount (X_1), incubation time (X_2), ultrasound power (X_3), and ultrasound time (X_4), which were consistent with the results of single-factor experiments (Fig. 2). Furthermore, by comparing the steepness of surfaces, it can be found that ultrasound power (X_3) elicited more obvious influences on CBPs yield, followed by incubation time (X_2), cellulase amount (X_1), and ultrasound time (X_4).

The accuracy of the present model was also confirmed by the predicted optimal experiment. The optimal conditions for CBPs extraction obtained from Design Expert software were: Cellulase amount of 0.71%, incubation time of 58.41 min, ultrasound power of 728.87 W, and ultrasound time of 29.51 min. Under these conditions, the predicted maximum yield of CBPs was 1.12%. To facilitate practical operation, the predicted extraction parameters were simplified to the following conditions: Cellulase amount of 0.7%, incubation time of 58 min, ultrasound power of 729 W, and ultrasound time of 30 min, under which the actual yield of CBPs was 1.17±0.06%, with an error of ±4.46% relative to the predicted value, which was less than ±5.0％, further confirming the accuracy of the present model (Zhang *et al*., 2019).

Comparisons of Different Extraction Methods

To explore the contributions of cellulase treatment and ultrasound irradiation to the CBPs yield, Hot-Water

Extraction (HWE, without cellulase and ultrasound), Enzyme-Assisted Extraction (EAE, without ultrasound), and ultrasound-assisted extraction (UAE, without cellulase) were conducted via fixing other parameters and compared with UAEE under the optimal conditions. As shown in Fig. 4, the CBPs yield with UAEE was remarkably higher ($P<0.01$) than with HWE, EAE, and UAE, respectively. As compared with HWE, notable differences were found in EAE ($P<0.05$) and UAE ($P<0.01$). The CBPs yield with UAE was a little higher than that with EAE ($0.79\pm0.10\%$ vs. $0.71\pm0.07\%$), but a significant difference ($P>0.05$) was not observed. These results implied that the cellulase treatment and/or ultrasound irradiation can significantly improve the yield of CBPs and the contribution of UAE is almost equivalent to that of EAE. The cavitation effects of ultrasound irradiation can generate high shear forces in the media to strengthen the cell wall-rupturing effects of cellulase (Chemat *et al*., 2017). Hence, when cellulase treatment was combined with ultrasound irradiation, CBPs yield achieved a relatively higher level of $1.17\pm0.06\%$ under optimal conditions.

Structural Characterization

After deproteinization and DEAE chromatographic purification, the polysaccharides content in CBPs reached $77.12\pm2.05\%$. As shown in Fig. 5, CBPs consisted of ribose, rhamnose, glucuronic acid, galacturonic acid, glucose, galactose, xylose, arabinose, and fructose at molar ratios of 3.82: 4.25: 3.54: 8.11: 32.89: 1.00: 27.96: 12.57: 13.25 (Fig. 5A) and possessed a molecular weight of 215.7 kDa (Fig. 5B). Corn silk as mentioned above is another by-product of corn production and processing. Previous publications revealed that Corn Silk Polysaccharides (CSPs) comprise rhamnose, arabinose, xylose, mannose, glucose, and galactose at molar ratios of 0.17: 0.30: 0.26: 0.35: 1.00: 0.57 and have molecular weights ranging from 586 to 813 kDa (Li *et al*., 2020; Zhao *et al*., 2017), which indicated that there are differences in the structural properties of polysaccharides from the corn silk compared with the corn bract. It may be associated with the fact that different organs of the same plant species generate different enzymes that catalyze the biosynthesis of different bio constituents, leading to a tissue-specific distribution of phytochemicals in the same plant (Tian *et al*., 2019).

As shown in Fig. 6A, the particle size of CBPs was around 255 nm, suggesting CBPs might assemble in water, which was also observed in the glucan polysaccharide from sweet potato (with a particle size of 230 nm) (Ji *et al*., 2021). The SEM image of CBPs was presented in Fig. 6B and the surface of CBPs appears to be full of holes and bumps. The surface appearance of holes and bumps are the characteristics of macromolecular polysaccharides, which may be caused by the hydrophobic interaction in polysaccharides (Yin *et al*., 2007).

The FT-IR spectrum of CBPs was exhibited in Fig. 7. The peak at 3432 cm^{-1} was attributed to the stretching vibration of -OH and the signals at 2925 and 2852 cm^{-1} were assigned to the stretching and bending vibrations of -CH$_2$- and -CH$_3$ and the symmetrical stretching vibration of -CH$_2$-, respectively (Acemi, 2020; Chen *et al*., 2019). The peaks at 1637 cm^{-1} and 1417 cm^{-1} were assigned to the asymmetric and symmetric stretching vibrations of -C=O in the carbonyl group. The signal at 1224 cm^{-1} was attributed to the vibration of -S=O in sulfate ester and the peak at 1074 cm^{-1} could be from the variable angle vibration of -OH in the C-O-H group (Trifan *et al*., 2015; Li *et al*., 2014). The signal at 599 cm^{-1} was consistent with the stretching vibration of O-S-O (Li *et al*., 2018). Therefore, the FT-IR analysis further verified that CBPs possess the typical characteristics of polysaccharides and could be a kind of naturally occurring sulfated polysaccharides.

The in Vitro Antioxidant Activities

Hydroxyl radical is the most Reactive Oxygen Species (ROS) that exerts the ability to react with almost any molecules in cells (Hou *et al*., 2020). While, DPPH radical is a relatively stable nitrogen-containing free radical and if the sample can quench it effectively, it might indicate that the sample has higher scavenging capability against Reactive Nitrogen Species (RNS) (Zheng *et al*., 2015). Thus, hydroxyl and DPPH radicals are usually widely selected to assess the antioxidant potential of tested samples.

From Fig. 8A, it can be seen that the hydroxyl radical-scavenging capacities of CBPs were enhanced with the concentrations of 0-5 mg.mL^{-1} in a concentration-dependent manner ($P<0.05$ or $P<0.01$). When concentration reached 5 mg.mL^{-1}, the hydroxyl radical-scavenging rate of CBPs was $93.47\pm3.68\%$, lower than that of LAA at the same concentration ($99.87\pm2.12\%$), but a significant difference was not observed ($P>0.05$). As shown in Fig. 8B, the DPPH radical-scavenging activities of CBPs were also increased in a concentration-dependent manner ($P<0.01$) within the concentrations ranging from 0 to 5 mg.mL^{-1}. When the concentration was 5 mg.mL^{-1}, the DPPH radical-scavenging rate of CBPs reached $85.12\pm3.32\%$, significantly lower ($P<0.01$) than that of LAA at the same concentration ($99.97\pm2.28\%$). The half-maximal inhibitory concentration (IC$_{50}$) of CBPs for scavenging DPPH radical was 2.30 ± 0.02 mg.mL^{-1}, significantly higher ($P<0.05$) than that of hydroxyl radical (1.76 ± 0.14 mg.mL^{-1}), indicating that CBPs has stronger scavenging capacities against hydroxyl radical than that of DPPH radical. In short, CBPs extracted under the optimal conditions of UAEE exhibit promising antioxidant potentials, especially for quenching ROS with advantage.

Previously published research uncovered that the Corn Silk Polysaccharides (CSPs) scavenged hydroxyl and DPPH radicals with IC$_{50}$ values of 0.46 ± 0.004 mg.mL^{-1} and 3.57 ± 0.005 mg.mL^{-1}, respectively (Li *et al*., 2020). When

compared with those of CBPs, it can be concluded that the hydroxyl radical-scavenging capacity of CBPs is stronger than that of CSPs, while the DPPH radical-scavenging capacity of CBPs is inferior to CSPs, further confirming the above consumption that CBPs preferentially scavenge ROS.

Table 2: The results of the RSM-BBD design

Run	Variables		Response		
	X_1	X_2	X_3	X_4	Y
1	0.7 (0)	70 (1)	600 (-1)	30 (0)	0.48
2	0.8 (1)	60 (0)	700 (0)	40 (1)	0.67
3	0.7 (0)	60 (0)	700 (0)	30 (0)	1.15
4	0.7 (0)	50 (-1)	700 (0)	40 (1)	0.88
5	0.8 (1)	50 (-1)	700 (0)	30 (0)	0.80
6	0.7(0)	60 (0)	700 (0)	30 (0)	1.05
7	0.6 (-1)	60 (0)	700 (0)	20 (-1)	0.60
8	0.7 (0)	60 (0)	700 (0)	30 (0)	1.08
9	0.7 (0)	60 (0)	700 (0)	30 (0)	1.10
10	0.6 (-1)	70 (1)	700 (0)	30 (0)	0.77
11	0.6 (-1)	60 (0)	600 (-1)	30 (0)	0.51
12	0.7 (0)	60 (0)	600 (-1)	40 (1)	0.55
13	0.7 (0)	70 (1)	700 (0)	20 (-1)	0.73
14	0.7 (0)	60 (0)	700 (0)	30 (0)	1.10
15	0.7 (0)	50 (-1)	600 (-1)	30 (0)	0.65
16	0.8 (1)	70 (1)	700 (0)	30 (0)	0.75
17	0.8 (1)	60 (0)	700 (0)	20 (-1)	0.93
18	0.6 (-1)	60 (0)	800 (1)	30 (0)	0.75
19	0.7 (0)	60 (0)	800 (1)	40 (1)	0.76
20	0.6 (-1)	60 (0)	700 (0)	40 (1)	0.79
21	0.7 (0)	50 (-1)	800 (1)	30 (0)	0.82
22	0.6 (-1)	50 (-1)	700 (0)	30 (0)	0.88
23	0.8 (1)	60 (0)	800 (1)	30 (0)	0.82
24	0.7 (0)	60 (0)	600 (-1)	20 (-1)	0.42
25	0.7 (0)	50 (-1)	700 (0)	20 (-1)	0.84
26	0.7 (0)	70 (1)	800 (1)	30 (0)	0.97
27	0.8 (1)	60 (0)	600 (-1)	30 (0)	0.44
28	0.7 (0)	60 (0)	800 (1)	20 (-1)	0.82
29	0.7 (0)	70 (1)	700 (0)	40 (1)	0.72

Table 3: The ANOVA for response surface quadratic model

Source	Sum of squares	df [a]	Mean square	*F*-value	*P*-value	Significance [b]
Model	1.0900	14	0.078	34.190	<0.0001	**
X_1	1.008×10^{-3}	1	1.008×10^{-3}	0.440	0.5165	n.s.
X_2	0.0170	1	0.017	7.410	0.0165	*
X_3	0.3000	1	0.300	130.760	<0.0001	**
X_4	7.50×10^{-5}	1	7.50×10^{-5}	0.033	0.8586	n.s.
X_1X_2	9.0×10^{-4}	1	9.0×10^{-4}	0.400	0.5396	n.s.
X_1X_3	4.9×10^{-3}	1	4.9×10^{-3}	2.150	0.1644	n.s.
X_1X_4	0.0510	1	0.051	22.240	0.0003	**
X_2X_3	0.0260	1	0.026	11.250	0.0047	**
X_2X_4	6.25×10^{-4}	1	6.25×10^{-4}	0.270	0.6085	n.s.
X_3X_4	9.03×10^{-3}	1	9.03×10^{-3}	3.960	0.0664	n.s.
X_1^2	0.2200	1	0.220	94.560	<0.0001	**
X_2^2	0.0780	1	0.078	34.270	<0.0001	**
X_3^2	0.4800	1	0.480	211.070	<0.0001	**
X_4^2	0.2200	1	0.220	94.560	<0.0001	**
Residual	0.0320	14	2.28×10^{-3}			
Lack of fit	0.0270	10	2.66×10^{-3}	2.000	0.2639	n.s.
Pure error	5.32×10^{-3}	4	1.33×10^{-3}			
Cor total	1.1200	28				
R^2	0.9716			Adjusted R^2	0.9432	

[a]Degree of freedom
[b]*P<0.05; **P<0.01; n.s. refers to "not significant"
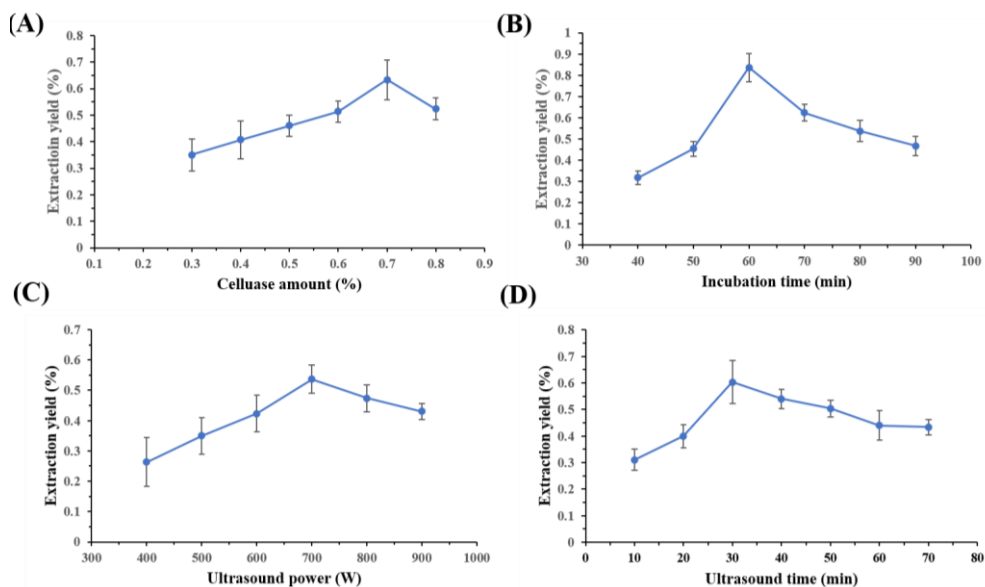
Fig. 2: The effects of cellulase amount (A), incubation time (B), ultrasound power (C), and ultrasound time (D) on CBPs yield. The data were presented as the means ± SD (n = 3)
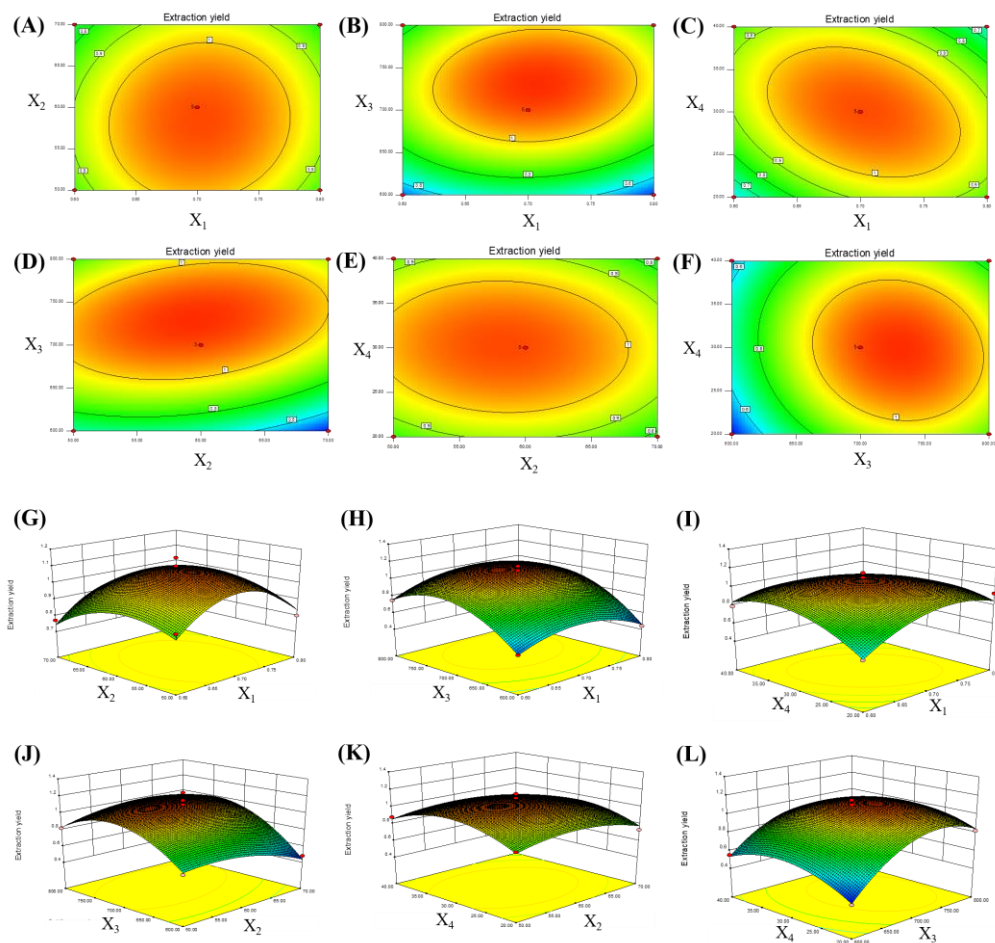
Fig. 3. The contour (A – F) and response surface plots (G-L) show the effects of variables on CBPs yield

245
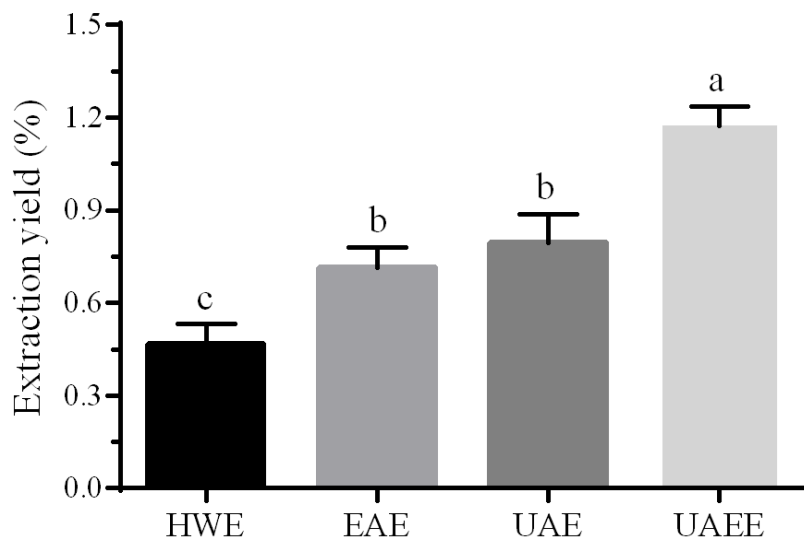
Fig. 4: The contributions of different extraction methods to the CBPs yield. Data were expressed as means ± SD. Different letters in lowercase mean significant differences (P<0.05, or P<0.01). HWE: hot-water extraction; EAE
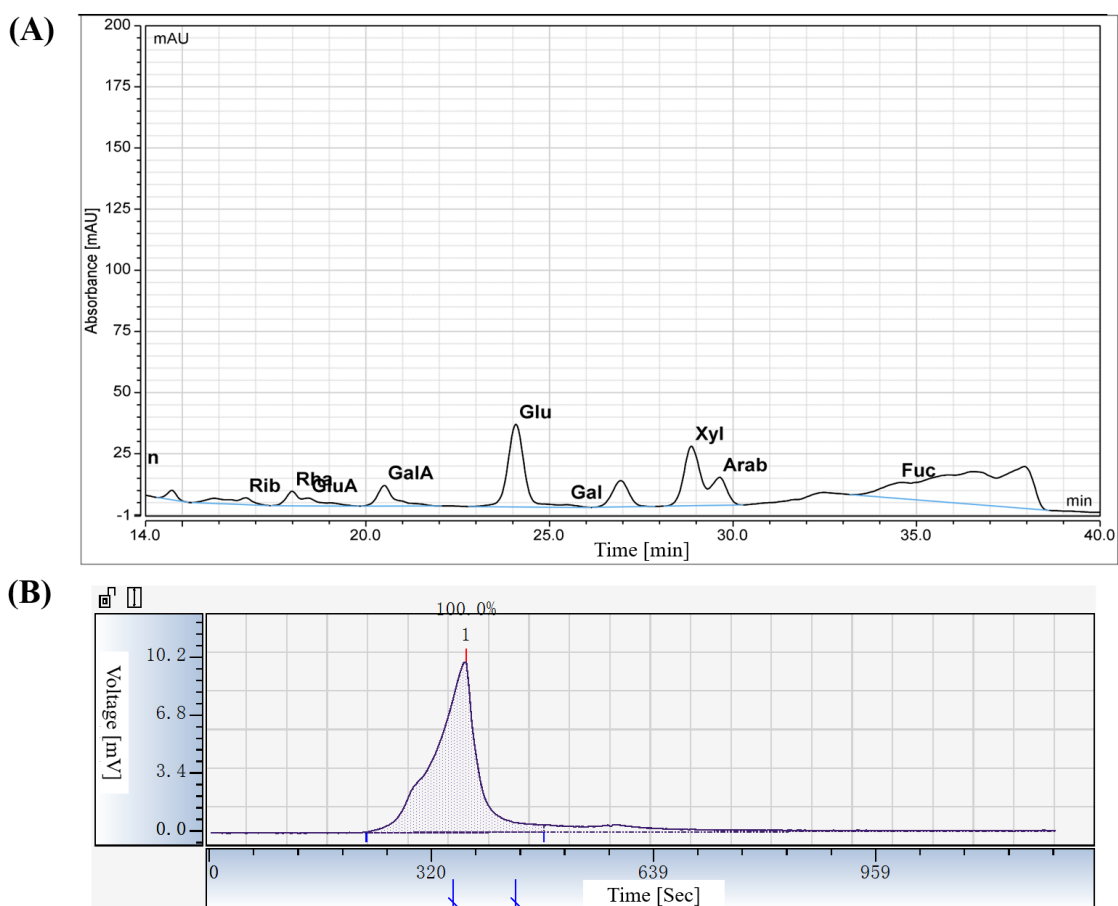
Fig. 5: The HPLC chromatogram of PMP-ladled monosaccharides (A) and HPSCE chromatogram (B) of CBPs. Rib: Ribose; Rha: Rhamnose; GluA: Glucuronic acid; GalA: Galacturonic acid; Glu: Glucose; Gal: Galactose; Xyl: Xylose; Arab: Arabinose; Fuc: Fructose
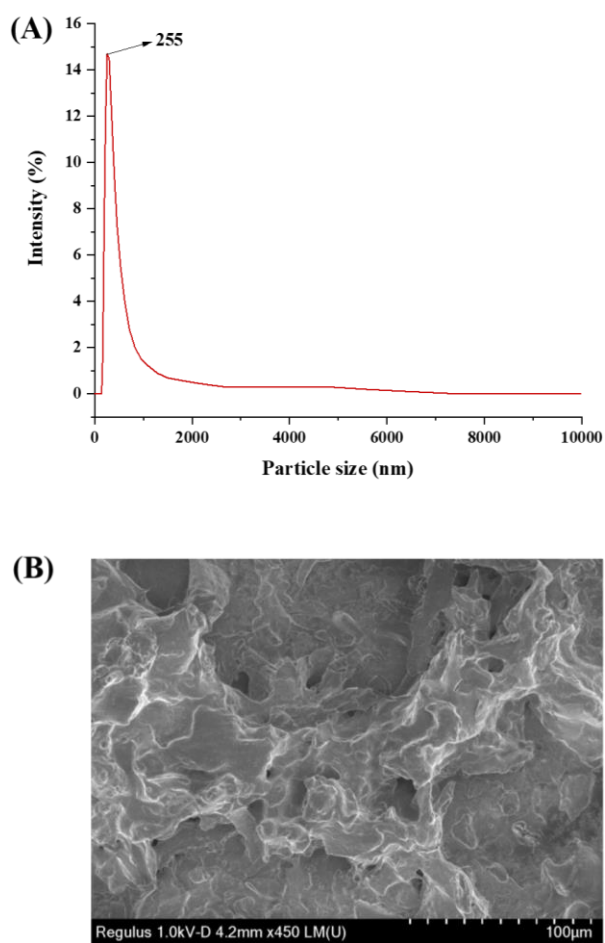
Fig. 6: The particle size (A) and SEM image (B) of CBPs
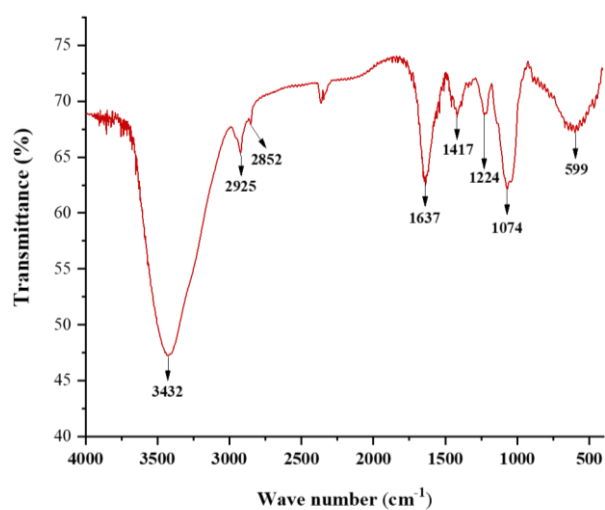
Fig. 7. FT-IR spectrum of CBPs
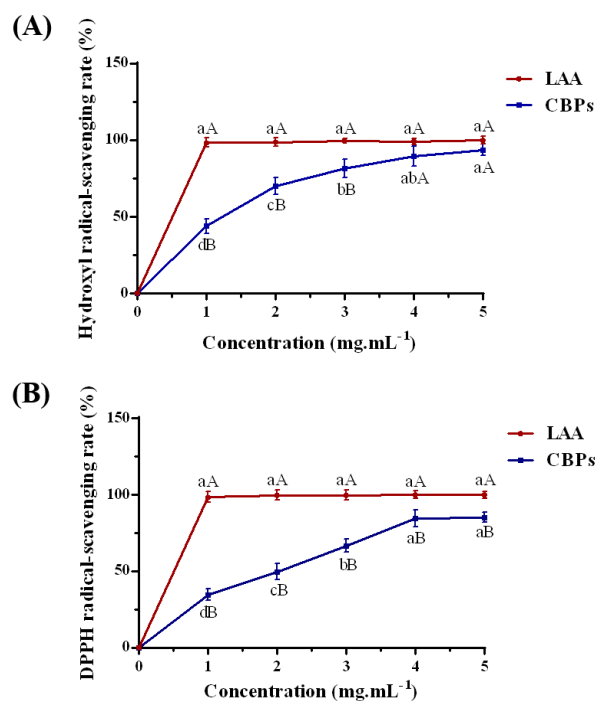
Fig. 8: The in vitro antioxidant potentials of CBPs using LAA as the positive control. (A) Hydroxyl radical-scavenging capacity; (B) DPPH radical-scavenging capacity. Different Letters in uppercase refer to significant differences (P<0.01) compared with LAA at the same concentration; Different letters in lowercase refer to significant differences (*P*<0.05, or *P*<0.01) within groups
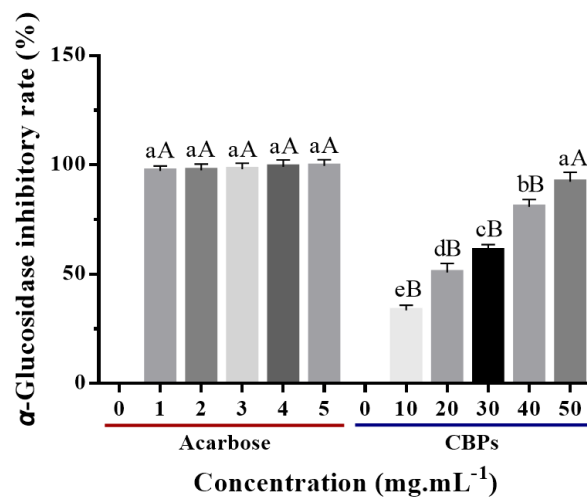
Fig. 9: The inhibitory effects of CBPs on α-glucosidase using acarbose as a positive control. Different letters in uppercase mean significant differences (*P*<0.01) between groups. Different letters in lowercase mean significant differences (*P*<0.01) within groups

The Inhibitory Effects on α-Glucosidase Activity

The α-glucosidase inhibitors are supposed as key factors for remedying type 2 diabetes, which can reduce the level of postprandial blood glucose effectively (Chen *et al.*, 2019). Currently, the inhibitory effects on glucosidase activity have been widely used to evaluate the *in vitro* hypoglycemic potential of natural polysaccharides.

As shown in Fig. 9, the inhibitory effects of CBPs on α-glucosidase increased in a concentration-dependent manner ($P<0.01$) within the concentrations of 0-50 mg.mL^{-1}. When the concentration reached 50 mg.mL^{-1}, the inhibition rate was 92.33±2.28%, still lower than that of acarbose (a marketed α-glucosidase inhibitor), which had reached 97.30±2.24% at a concentration of 1 mg.mL^{-1}. The IC$_{50}$ of CBPs for inhibiting α-glucosidase was 20.66±0.98 mg.mL^{-1}, higher than that of CSPs (1.62±0.03-7.75±0.05 mg.mL^{-1}) (Jia *et al.*, 2021). It is suggested that the inhibitory effect of CBPs on α-glucosidase is weaker than that of CSPs and the hypoglycemic potential of CBPs could be medium, not very high.

Conclusion

Corn bract is the main agricultural waste of corn production and processing, accounting for approximately 40% per unit area of corn cultivation. In our previous work, we explored the flavonoids from waste corn bract (Zhang *et al*., 2019). In the present study, we explored the Ultrasound-Assisted Enzymatic Extraction (UAEE) of Corn Bract Polysaccharides (CBPs) for the first time. Under the optimized UAEE, the CBPs yield reached 1.17±0.06% which was significantly higher ($P<0.01$) than those of Hot-Water Extraction (HWE), Enzyme-Assisted Extraction (EAE), and Ultrasound-Assisted Extraction (UAE), and the contribution of ultrasound irradiation to CBPs yield is similar to that of cellulase treatment. The CBPs extracted with UAEE are heteropolysaccharides consisting of ribose, rhamnose, glucuronic acid, galacturonic acid, glucose, galactose, xylose, arabinose, and fructose with glucose the largest proportion and having the relatively larger molecular weight and particle size. The SEM and FT-IR analyses further confirmed that the structures of CBPs accord with the characteristics of polysaccharides and could be a kind of naturally occurring sulfated polysaccharides, which is pending to be further verification. Moreover, CBPs preferentially quench Reactive Oxygen Species (ROS) and the hydroxyl radical-scavenging capacity of CBPs is stronger than that of Corn Silk Polysaccharides (CSPs), but the α-glucosidase inhibiting effect is inferior to CSPs. Yet despite all this, CSPs extracted with the optimized UAEE still have certain potentials to treat type 2 diabetes via inhibiting α-glucosidase, which deserves further investigations. In the next study, the fine structural characteristics of CSPs, including the type and sequence of monosaccharides, the repeating units, and the degree of branching, should be considered to better elucidate the underlying structure-activity relationships.

Author's Contributions

Yihui Liu, Yayi Li and Yuxing Xie: Optimized the extraction process.

Wangyou Zhang, Shuaiyi Dong and Na Niu: Characterized the structures.

Gulei Pu, Chenqi Liu and Caibo Jiang: Performed the experiments of in vitro antioxidant and hypoglycemic evaluations.

Yang Liu and Yang Zhang: Conceived and designed the experiments and financed the project.

Mingjin Cai: Processed the data.

Ethics

This article is original and contains unpublished material. The corresponding author confirms that all of the other authors have read and approved the manuscript and no ethical issues involved.

References

Azcarate, S. M., Pinto, L., & Goicoechea, H. C. (2020). Applications of mixture experiments for response surface methodology implementation in analytical methods development. Journal of Chemometrics, 34(12), e3246. doi.org/10.1002/cem.3246

Acemi, A. (2020). The polymerization degree of chitosan affects structural and compositional changes in the cell walls, membrane lipids and proteins in the leaves of Ipomoea purpurea: An FT-IR spectroscopy study. International Journal of Biological Macromolecules, 162, 715-722.
doi.org/10.1016/j.ijbiomac.2020.06.171

Andreadi, A., Bellia, A., Di Daniele, N., Meloni, M., Lauro, R., Della-Morte, D., & Lauro, D. (2022). The molecular link between oxidative stress, insulin resistance and type 2 diabetes: A target for new therapies against cardiovascular diseases. Current Opinion in Pharmacology, 62, 85-96. doi.org/10.1016/j.coph.2021.11.010

Chemat, F., Rombaut, N., Sicaire, A. G., Meullemiestre, A., Fabiano-Tixier, A. S., & Abert-Vian, M. (2017). Ultrasound assisted extraction of food and natural products. Mechanisms, techniques, combinations, protocols and applications. A review. Ultrasonics sonochemistry, 34, 540-560. doi.org/10.1016/j.ultsonch.2016.06.035

Chen, J., Zhang, X., Huo, D., Cao, C., Li, Y., Liang, Y., & Li, L. (2019). Preliminary characterization, antioxidant and α-glucosidase inhibitory activities of polysaccharides from Mallotus furetianus. Carbohydrate Polymers, 215, 307-315. doi.org/10.1016/j.carbpol.2019.03.099

Chen, R., Li, S., Liu, C., Yang, S., & Li, X. (2012). Ultrasound complex enzymes assisted extraction and biochemical activities of polysaccharides from Epimedium leaves. Process Biochemistry, 47(12), 2040-2050. doi.org/10.1016/j.procbio.2012.07.022

Chen, S., Xing, X. H., Huang, J. J., & Xu, M. S. (2011). Enzyme-assisted extraction of flavonoids from Ginkgo biloba leaves: Improvement effect of flavonol trans glycosylation catalyzed by Penicillium decumbens cellulase. Enzyme and microbial technology, 48(1), 100-105. doi.org/10.1016/j.enzmictec.2010.09.017

Chzhu, O. P., Araviashvili, D. E., & Danilova, I. G. (2020). Studying properties of prospective biologically active extracts from Marine Hydrobionts. Emerg. Sci. J, 4(1), 37-43. doi.org/10.28991/esj-2020-01208

Dubois, M., Gilles, K. A., Hamilton, J. K., Rebers, P. T., & Smith, F. (1956). Colorimetric method for determination of sugars and related substances. Analytical chemistry, 28(3), 350-356. doi.org/10.1021/ac60111a017

Fu, Y. J., Liu, W., Zu, Y. G., Tong, M. H., Li, S. M., Yan, M. M., & Luo, H. (2008). Enzyme assisted extraction of luteolin and apigenin from pigeonpea [*Cajanuscajan* (L.) Millsp.] leaves. Food Chemistry, 111(2), 508-512. doi.org/10.1016/j.foodchem.2008.04.003

Gesteiro, N., Butrón, A., Estévez, S. & Santiago, R. (2021). Unraveling the role of maize (zea mays l.) cell-wall phenylpropanoids in stem-borer resistance. Phytochemistry, 185, 112683. doi.org/10.1016/j.phytochem.2021.112683

Hasanudin, K., Hashim, P., & Mustafa, S. (2012). Corn silk (Stigma maydis) in healthcare: A phytochemical and pharmacological review. Molecules, 17(8), 9697-9715. doi.org/10.3390/molecules17089697

Hou, J. T., Zhang, M., Liu, Y., Ma, X., Duan, R., Cao, X., & Ren, W. X. (2020). Fluorescent detectors for hydroxyl radical and their applications in bioimaging: A review. Coordination Chemistry Reviews, 421, 213457. doi.org/10.1016/j.ccr.2020.213457

Hu, Z., Zhou, H., Li, Y., Wu, M., Yu, M., & Sun, X. (2019). Optimized purification process of polysaccharides from Carex meyeriana Kunth by macroporous resin, its characterization and immunomodulatory activity. International journal of biological macromolecules, 132, 76-86. doi.org/10.1016/j.ijbiomac.2019.03.207

Huang, D., Zhou, X., Si, J., Gong, X., & Wang, S. (2016). Studies on cellulase-ultrasonic assisted extraction technology for flavonoids from Illicium verum residues. Chemistry Central Journal, 10(1), 1-9. doi.org/10.1186/s13065-016-0202-z

Ismy, J., Syukri, M., Emril, D. R., Sekarwana, N., & Ismy, J. (2022). Superoxide Dismutase Reduces Creatinine and NGAL by Restoring Oxidative Balance during Sepsis. Emerging Science Journal, 6(2), 286-294. doi.org/10.28991/ESJ-2022-06-02-06

Mason J, T., Chemat, F., & Vinatoru, M. (2011). The extraction of natural products using ultrasound or microwaves. Current Organic Chemistry, 15(2), 237-247. doi.org/10.2174/138527211793979871

Ji, C., Zhang, Z., Zhang, B., Chen, J., Liu, R., Song, D., & Guo, S. (2021). Purification, characterization and in vitro antitumor activity of a novel glucan from the purple sweet potato *Ipomoea Batatas* (L.) Lam. Carbohydrate Polymers, 257, 117605. doi.org/10.1016/j.carbpol.2020.117605

Ji, X., Peng, Q., Yuan, Y., Shen, J., Xie, X., & Wang, M. (2017). Isolation, structures and bioactivities of the polysaccharides from jujube fruit (Ziziphus jujuba Mill). A review. Food chemistry, 227, 349-357. doi.org/10.1016/j.foodchem.2017.01.074

Jia, Y., Xue, Z., Wang, Y., Lu, Y., Li, R., Li, N., & Chen, H. (2021). Chemical structure and inhibition on α-glucosidase of polysaccharides from corn silk by fractional precipitation. Carbohydrate polymers, 252, 117185. doi.org/10.1016/j.carbpol.2020.117185.

Jiang, Z., Wang, Y., Xiang, D., & Zhang, Z. (2022). Structural properties, antioxidant and hypoglycemic activities of polysaccharides purified from pepper leaves by high-speed counter-current chromatography. Journal of Functional Foods, 89, 104916. doi.org/10.1016/j.jff.2021.104916

Krishnamoorthi, R., Bharathakumar, S., Malaikozhundan, B., & Mahalingam, P. U. (2021). Microfabrication of gold nanoparticles: Optimization, characterization, stabilization and evaluation of its antimicrobial potential on selected human pathogens. Biocatalysts and Agricultural Biotechnology, 35, 102107. doi.org/10.1016/j.bcab.2021.102107

Krishnamoorthi, R., Mahalingam, P. U., & Malaikozhundan, B. (2022). Edible mushroom extract engineered Ag NPs as safe antimicrobial and antioxidant agents with no significant cytotoxicity on human dermal fibroblast cells. Inorganic Chemistry Communications, 139, 109362. doi.org/10.1016/j.inoche.2022.109362

Li, L., Li, X., Ding, C., Yuan, S., Zhang, Z., Chen, Y., & Yuan, M. (2016). Ultrasonic-assisted enzymatic extraction and antioxidant activity of polysaccharides from Setaria viridis. Separation Science and Technology, 51(11), 1798-1805. doi.org/10.1080/01496395.2016.1178287

Li, X. L., Tu, X. F., Thakur, K., Zhang, Y. S., Zhu, D. Y., Zhang, J. G., & Wei, Z. J. (2018). Effects of different chemical modifications on the antioxidant activities of polysaccharides sequentially extracted from peony seed dreg. International journal of biological macromolecules, 112, 675-685. doi.org/10.1016/j.ijbiomac.2018.01.216

Li, X. L., Xiao, J. J., Zha, X. Q., Pan, L. H., Asghar, M. N., & Luo, J. P. (2014). Structural identification and sulfated modification of an antiglycation Dendrobium huoshanense polysaccharide. Carbohydrate polymers, 106, 247-254. doi.org/10.1016/j.carbpol.2014.02.029

Li, Y., Hu, Z., Wang, X., Wu, M., Zhou, H., & Zhang, Y. (2020). Characterization of a polysaccharide with antioxidant and anti-cervical cancer potentials from the corn silk cultivated in Jilin province. International journal of biological macromolecules, 155, 1105-1113. doi.org/10.1016/j.ijbiomac.2019.11.077

Luo, T., Tian, X., Yang, C., Luo, W., Nie, Y., & Wang, Y. (2017). Polyethylenimine-functionalized corn bract, an agricultural waste material, for efficient removal and recovery of Cr (VI) from aqueous solution. Journal of agricultural and food chemistry, 65(33), 7153-7158. doi.org/10.1021/acs.jafc.7b02699

Lv, Q. Q., Cao, J. J., Liu, R., & Chen, H. Q. (2021). Structural characterization, α-amylase and α-glucosidase inhibitory activities of polysaccharides from wheat bran. Food Chemistry, 341, 128218. doi.org/10.1016/j.foodchem.2020.128218

Ni, G., Hu, Z., Wang, Z., Zhang, M., Liu, X., Yang, G., & Zhang, Y. (2022). Cysteine donor-based brain-targeting prodrug: Opportunities and challenges. Oxidative medicine and cellular longevity, 2022. doi.org/10.1155/2022/4834117

Peng, K. Z., Zhang, S. Y., & Zhou, H. L. (2016). Toxicological evaluation of the flavonoid-rich extract from maydis stigma: Subchronic toxicity and genotoxicity studies in mice. Journal of Ethno pharmacology, 192, 161-169. doi.org/10.1016/j.jep.2016.07.012

Tian, H., Zhao, H., Zhou, H., & Zhang, Y. (2019). Chemical composition and antimicrobial activity of the essential oil from the aerial part of Dictamnus dasycarpus Turcz. Industrial crops and products, 140, 111713. doi.org/10.1016/j.indcrop.2019.111713

Trifan, A., Daciana, S. A. V. A., Bucur, L., Vasincu, A., Vasincu, I., Aprotosoaie, A. C., & Miron, A. (2015). Isolation, characterization and antioxidant activity of the crude polysaccharide from Phyllophora pseudoceranoides. The Medical-Surgical Journal, 119(2), 603-609.

Umana, U. S., Ebong, M. S., & Godwin, E. O. (2020). Biomass production from oil palm and its value chain. Journal of Human, Earth and Future, 1(1), 30-38. doi.org/10.28991/HEF-2020-01-01-04

Vo, T. S., & Kim, S. K. (2014). Marine-derived polysaccharides for regulation of allergic responses. Advances in food and nutrition research, 73, 1-13. doi.org/10.1016/B978-0-12-800268-1.00001-9

Wang, Z., Wang, Z., Huang, W., Suo, J., Chen, X., Ding, K., & Zhang, H. (2020). Antioxidant and anti-inflammatory activities of an anti-diabetic polysaccharide extracted from Gynostemma pentaphyllum herb. International journal of biological macromolecules, 145, 484-491. doi.org/10.1016/j.ijbiomac.2019.12.213

Wei, E., Yang, R., Zhao, H., Wang, P., Zhao, S., Zhai, W., & Zhou, H. (2019). Microwave-assisted extraction releases the antioxidant polysaccharides from seabuckthorn (*Hippophae rhamnoides* L.) berries. International journal of biological macromolecules, 123, 280-290. doi.org/10.1016/j.ijbiomac.2018.11.074

Wu, H., Zhu, J., Diao, W., & Wang, C. (2014). Ultrasound-assisted enzymatic extraction and antioxidant activity of polysaccharides from pumpkin (Cucurbita moschata). Carbohydrate polymers, 113, 314-324. doi.org/10.1016/j.carbpol.2014.07.025

Yang, D., Zhou, Z., & Zhang, L. (2019). An overview of fungal glycan-based therapeutics. Progress in Molecular Biology and Translational Science, 163, 135-163.

Yin, Y., Zhang, H., & Nishinari, K. (2007). Voltammetric characterization on the hydrophobic interaction in polysaccharide hydrogels. The Journal of Physical Chemistry B, 111(7), 1590-1596. doi.org/10.1021/jp0660334

Zhang, Y., Liu, Y., Zhu, K., Dong, Y., Cui, H., Mao, L., & Zhou, H. (2018). Acute toxicity, antioxidant and antifatigue activities of protein-rich extract from Oviductus ranae. Oxidative Medicine and Cellular Longevity, 2018. doi.org/10.1155/2018/9021371

Zhang, Y., Lu, J., Ben, L. J., Zheng, L. X., Xu, P. F., Jia, Y. G., Chen, Z. Y., & Yan, Z. W. (2019). Optimization of cellulase-assisted extraction of total flavonoids from corn bract and evaluation of antioxidant and antibacterial activities. Am. J. Biochem. Biotechnol., 15(2), 61-74. doi.org/10.3844/ajbbsp.2019.61.74

Zhang, Y., Yang, G., Wang, X., Ni, G., Cui, Z., & Yan, Z. (2021). Sagittaria trifolia tuber: Bioconstituents, processing, products, and health benefits. Journal of the Science of Food and Agriculture, 101(8), 3085-3098. doi.org/10.1002/jsfa.10977

Zhang, Y., Xu, H., Hu, Z. B., Yang, G. H., Yu, X. J., Chen, Q. F., Zheng, L. X. & Yan, Z. W. (2022) Eleocharis dulcis corm: Phytochemicals, health benefits, processing and food products. Journal of the Science of Food and Agriculture, 102(1), 19-40. doi.org/10.1002/ jsfa.11508

Zhao, H. P., Zhang, Y., Liu, Z., Chen, J. Y., Zhang, S. Y., Yang, X. D., & Zhou, H. L. (2017). Acute toxicity and anti-fatigue activity of polysaccharide-rich extract from corn silk. Biomedicine and Pharmacotherapy, 90, 686-693. doi.org/10.1016/j.biopha.2017.04.045

Zheng, L., Lin, L., Su, G., Zhao, Q., & Zhao, M. (2015). Pitfalls of using 1, 1-diphenyl-2-picrylhydrazyl (DPPH) assay to assess the radical scavenging activity of peptides: Its susceptibility to interference and low reactivity towards peptides. Food Research International, 76, 359-365. doi.org/10.1016/j.foodres.2015.06.045